Complex II Subunit SDHD is Critical for Cell Growth and Metabolism, Which can be Partially Restored with A Synthetic Ubiquinone Analog

Aloka B Bandara (abandara@vt.edu)
Virginia Tech
David A Brown
Mitochondrial Solutions
Joshua Drake
Virginia Tech: Virginia Polytechnic Institute and State University

Research article

Keywords: Electron transport chain, Complex II, Krebs cycle, succinate dehydrogenase, SDHD, CRISPR/Cas9, respiration, oxygen consumption, glycolysis, ATP synthesis, apoptosis, necrosis, ROS, idebenone.

Posted Date: November 20th, 2020

DOI: https://doi.org/10.21203/rs.3.rs-111135/v1

Complex II subunit SDHD is critical for cell growth and metabolism, which can be partially restored with a synthetic ubiquinone analog

Aloka B. Bandara[1*], Joshua C. Drake[1], and David A. Brown[2]

[1]Department of Human Nutrition, Foods & Exercise, Virginia Tech, Blacksburg, VA 24061-0913, and [2]Mitochondrial Solutions, LLC, 800 Draper Road, Blacksburg VA 24060.

[*]Corresponding author:

1034 ILSB, 1981 Kraft Drive, Blacksburg VA 24061-0913

Phone: 540-231-0949

Email: abandara@vt.edu

ABSTRACT

Background: Succinate dehydrogenase (Complex II) plays a dual role in respiration by catalyzing the oxidation of succinate to fumarate in the mitochondrial Krebs cycle and transferring electrons from succinate to ubiquinone in the mitochondrial electron transport chain (ETC). Mutations in Complex II are associated with a number of pathologies. SDHD, one of the four subunits of Complex II, serves by anchoring the complex to the inner-membrane and transferring electrons from the complex to ubiquinone. Thus, modeling SDHD dysfunction could be a valuable tool for understanding its importance in metabolism and developing novel therapeutics, however no suitable models exist.

Results: Via CRISPR/Cas9, we mutated SDHD in HEK293 cells and investigated the *in vitro* role of SDHD in metabolism. Compared to the parent HEK293, the knockout mutant HEK293Δ*SDHD* produced significantly less number of cells in culture. The mutant cells predictably had suppressed Complex II-mediated mitochondrial respiration, but also Complex I-mediated respiration. SDHD mutation also adversely affected glycolytic capacity and ATP synthesis. Mutant cells were more apoptotic and susceptible to necrosis. Treatment with the mitochondrial therapeutic idebenone partially improved oxygen consumption and growth of mutant cells.

Conclusions: Overall, our results suggest that SDHD is vital for growth and metabolism of mammalian cells, and that respiratory and growth defects can be partially restored with treatment of a ubiquinone analog. This is the first report to use CRISPR/Cas9 approach to construct a knockout SDHD cell line and evaluate the efficacy of an established mitochondrial therapeutic candidate to improve bioenergetic capacity.

KEYWORDS

Electron transport chain, Complex II, Krebs cycle, succinate dehydrogenase, SDHD, CRISPR/Cas9, respiration, oxygen consumption, glycolysis, ATP synthesis, apoptosis, necrosis, ROS, idebenone.

1. INTRODUCTION

Mitochondria generate the majority of adenosine triphosphate (ATP) through the electron transport chain (ETC). Succinate dehydrogenase (Complex II; EC 1.3.5.1) uniquely serves as a component of both the Krebs cycle and the ETC [1, 2]. As a component of the Krebs Cycle, Complex II catalyzes oxidation of succinate to fumarate [1, 3], whereas in the ETC, it is one of two entry points for electrons, acquiring electrons from succinate and donating them to ubiquinone (CoQ) [1-3]. Thus, impairments in Complex II function can have severe consequences for maintaining energetic homeostasis. Mutations in Complex II subunits have been found in patients with mitochondrial respiratory deficiency [4], as well as a number of cancers [5-7]. Therefore, an in-depth understanding of Complex II in energetic homeostasis and its viability as a target for treatment is warranted.

Complex II carries four protein subunits [2], all of which are encoded by nuclear genes. Two subunits, SDHA and SDHB, are localized on the matrix side of the inner membrane, and carry the binding site for succinate, three FeS clusters, as well as a flavoprotein bound to an FAD cofactor [8]. The two remaining subunits, SDHC and SDHD, are hydrophobic and anchor the complex to the inner-membrane. Subunits SDHC and SDHD form the CoQ binding site of Complex II and serve as terminal electron transfers from Complex II to CoQ. In particular, mutation of SDHD has been noted in patients with paragangliomas and pheochromocytomas [7]. Therefore, given the particular role of SDHD in anchoring Complex II to the inner-membrane, passaging electrons to CoQ, and noted pathologies, modeling SDHD dysfunction could be a valuable tool for understanding the role of Complex II in metabolism and developing novel therapeutics. To date, however, suitable models for molecular examinations of any Complex II subunit do not exist.

We successfully used a CRISPR/cas9 approach to mutate the SDHD subunit of Complex II in HEK293 cells, and characterized its requirement for mitochondrial respiration, ATP synthesis, and

cell growth *in vitro*. Furthermore, we demonstrate the efficacy of the mitochondrial therapeutic idebenone to improve mitochondrial dysfunction in cells with SDHD mutation. Our results demonstrate the necessity of SDHD for energetic homeostasis and suggests it as a viable target for therapies aimed to improve mitochondrial function.

2. RESULTS

2.1. Construction of mutant HEK293Δ*SDHD*. The single guide RNA (sgRNA) sequences were designed based on the 609 bp long *SDHD* nucleotide sequence of *Homo sapiens* (GenBank locus ID KR710199.1) using Integrated DNA Technologies' online tool (Skokie, IL; https://www.idtdna.com/site/order/designtool/index/CRISPR_CUSTOM). A 118-bp site of the forward strand of *SDHD* was predicted as the most reliable for mutation. The guide strand predicted was TCTGTTGCTTCGAACTCCAG, which is located right upstream of the protospacer adjacent motif (PAM) sequence TGG (Fig. 1A). The constructed mutant HEK293Δ*SDHD* was validated by Western immunoblotting. The predicted molecular weight of SDHD is approximately

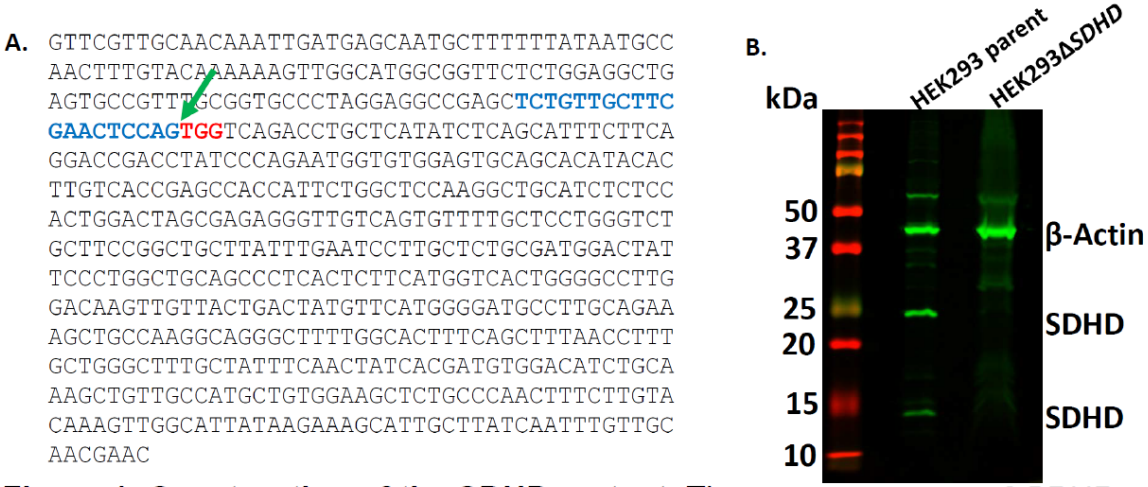

Figure 1. Construction of the SDHD mutant. The gene sequence of *SDHD* with CRISPR targeting sites is shown (A). The sgRNA and PAM sequences predicted by the online idtdna program are depicted in blue and red colors, respectively; the specific site for mutation (at 118-bp) is shown with a green arrow. Expression of SDHD protein is shown (B). The protein extracts reacted with rabbit polyclonal antibodies to SDHD and rabbit polyclonal antibodies to β-Actin are shown.

17 kDa. Nevertheless, the antibody used for mutant validation was anticipated to produce an additional band of about 29 kDa as well on the blot from parent cells (see the details from the vendor: https://www.lsbio.com/antibodies/cbt1-antibody-sdhd-antibody-n-terminus-wb-western-ls-c345301/356234). Our mutant HEK293Δ*SDHD* was found missing both 17 kDa and 29 kDa protein bands (Fig. 1B).

2.2. Loss of SDHD increases apoptosis and necrosis. Compared to the parent HEK293, the mutant HEK293Δ*SDHD* produced significantly increased amount of ROS at 0 h (immediately after addition of the substrate to the reaction; $p = 0.0128$; Fig. 2A). Nevertheless, the mutant produced significantly decreased ROS amounts at 24 h ($p = 0.0035$) and 72 h ($p < 0.0001$) after addition of the substrate. These observations suggest that disruption of *SDHD* results in subsequent

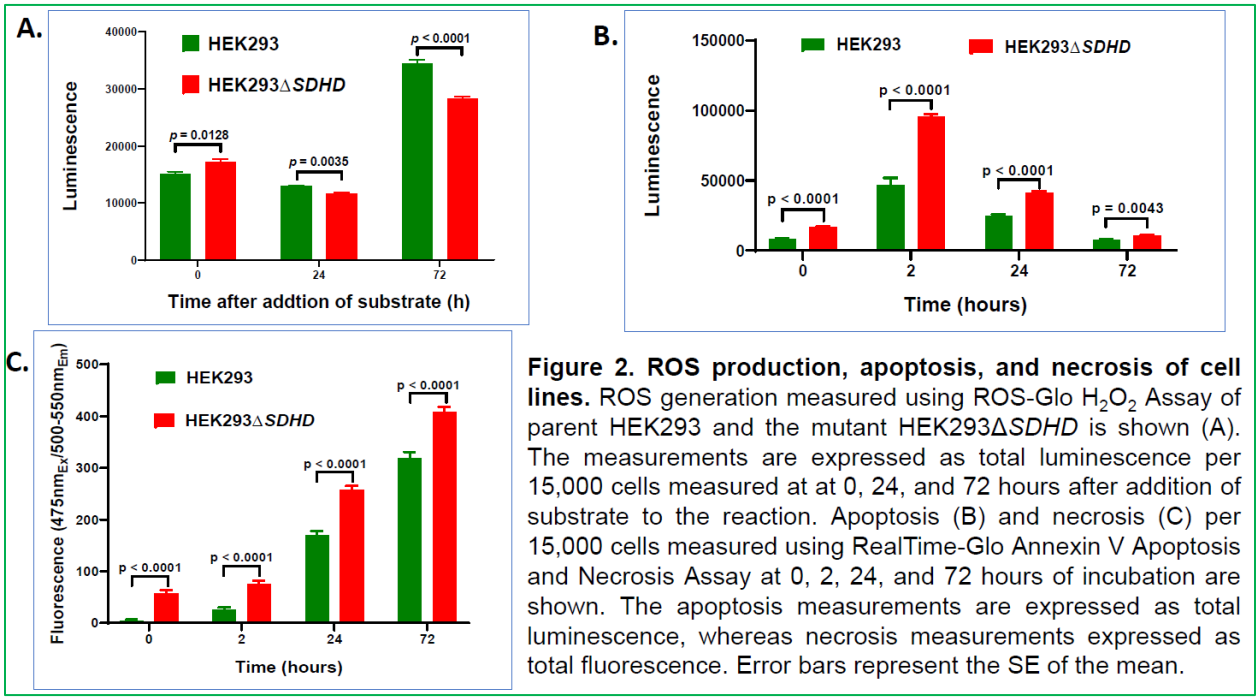

Figure 2. ROS production, apoptosis, and necrosis of cell lines. ROS generation measured using ROS-Glo H_2O_2 Assay of parent HEK293 and the mutant HEK293Δ*SDHD* is shown (A). The measurements are expressed as total luminescence per 15,000 cells measured at at 0, 24, and 72 hours after addition of substrate to the reaction. Apoptosis (B) and necrosis (C) per 15,000 cells measured using RealTime-Glo Annexin V Apoptosis and Necrosis Assay at 0, 2, 24, and 72 hours of incubation are shown. The apoptosis measurements are expressed as total luminescence, whereas necrosis measurements expressed as total fluorescence. Error bars represent the SE of the mean.

decrease of ROS generation over time. At all the time points, the mutant displayed significantly increased apoptosis ($p < 0.0001$, < 0.0001, < 0.0001, and $= 0.0043$ respectively at 0, 2, 24, and 72 h post-incubation; Fig. 2B). The mutant also showed significantly increased necrosis ($p <$

0.0001 for each time point; Fig. 2C). Our findings indicate that disruption of *SDHD* made the cells more apoptotic and susceptible to necrosis.

2.3. Loss of SDHD impairs growth. After four days of incubation in growth media, the number of cells recovered from the mutant HEK293Δ*SDHD* culture was ~73% less than the amount recovered from parent HEK293 culture ($p = 0.0002$; Fig 3A). The doubling of mutant over 4 days was significantly slower compared to that of the parent during the same duration of growth ($p = 0.0008$; Fig. 3B), suggesting that SDHD is vital for cell growth.

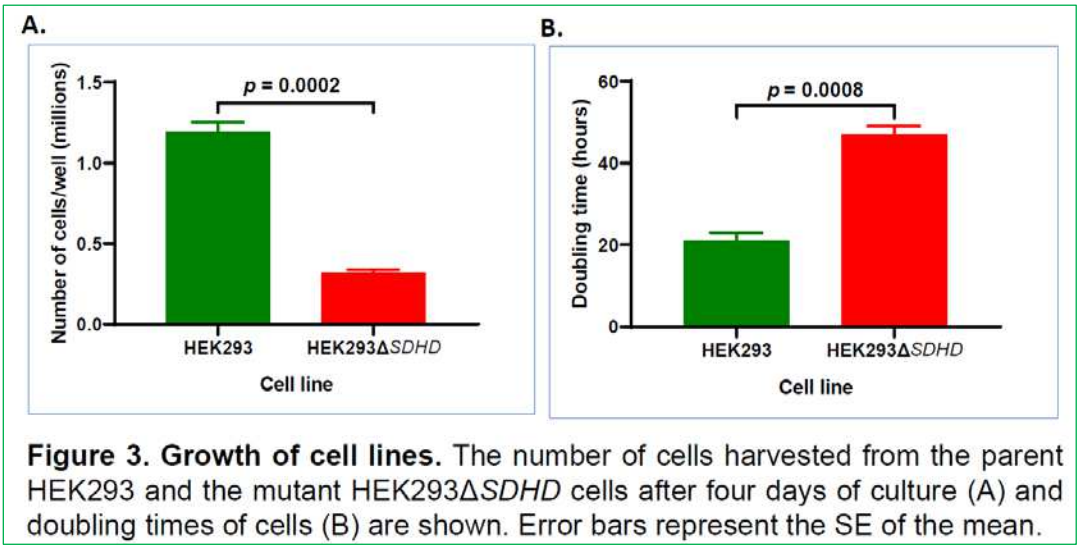

Figure 3. Growth of cell lines. The number of cells harvested from the parent HEK293 and the mutant HEK293Δ*SDHD* cells after four days of culture (A) and doubling times of cells (B) are shown. Error bars represent the SE of the mean.

2.4. Loss of SDHD impairs mitochondrial respiration Oxygen consumption was measured using Oroboros Oxygraph 2k. Mutation in SDHD decreased oxygen consumption all along the ETC (Fig. 4A). Complex I respiration was significantly decreased in mutant cells compared to parent ($p = 0.0019$). Subsequent to rotenone treatment, oxygen consumption of both parent and mutant decreased, but the oxygen consumption of mutant cells was significantly less than that of parent cells ($p = 0.0101$). In response to treatment with succinate, Complex II-mediated oxygen consumption was significantly repressed in mutant cells compared to parent cells ($p = 0.0002$), further confirming the effect SDHD mutation. The mutant also had decreased OXPHOS capacity ($p = 0.0002$) and maximal respiration ($p = 0.0017$). Oxygen consumption of permeabilized cells

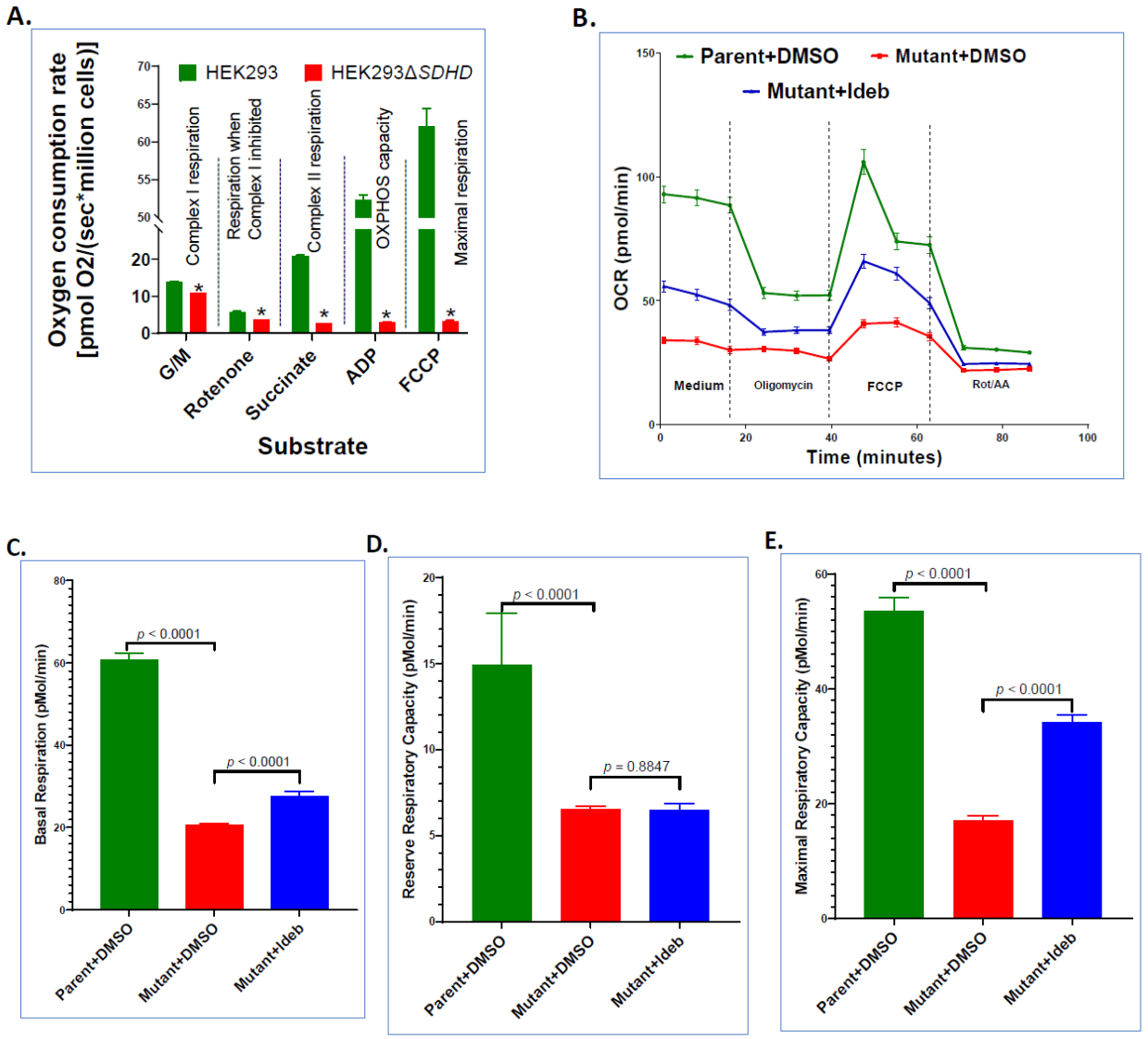

Figure 4. Respiration, of cell lines. Oxygen consumption rates measured using Oroboros O2k per million cells in response to treatment with glutamate-malate (G/M), rotenone, succinate, ADP, and FCCP (A) are shown. The mean oxygen consumption rates were compared between the parent HEK293 and the mutant HEK293Δ*SDHD*. The *p* values for the differences between the mean values were 0.0019, 0.0101, 0.0002, 0.0002, and 0.0017, respectively for Complex I respiration, rotenone treatment, Complex II respiration, OXPHOS capacity, and maximal respiration. Oxygen consumption rate (OCR) was measured using Agilent Seahorse XFe96 of parent cells treated DMSO (Parent+DMSO), mutant cells treated DMSO (Mutant+DMSO), and mutant cells treated 1μM idebenone (Mutant+Ideb). OCR per 20,000 permeabilized cells (B), and the calculated basal respiration (C), reserve respiratory capacity (D) and maximal respiratory capacity (E) are shown. The mean OCR values were compared between the parent versus the mutant or DMSO treatment versus idebenone treatment. Error bars represent the SE of the mean.

was also assessed using an Agilent Seahorse XFe96 Analyzer (Fig 4B). In the mutant, basal respiration ($p < 0.0001$; Fig. 4C), reserve respiratory capacity ($p < 0.0001$; Fig 4D), and maximal

respiratory capacity ($p < 0.0001$; Fig. 4E) decreased significantly. Oroboros O2k and Seahorse OCR assays collectively indicate a severe impairment of cellular respiration due to SDHD disruption.

2.5. Loss of SDHD impairs glycolytic capacity and ATP synthesis of cell lines. ECAR of intact cells was determined using an Agilent Seahorse XFe96 Analyzer (Fig. 5A). Both glycolysis

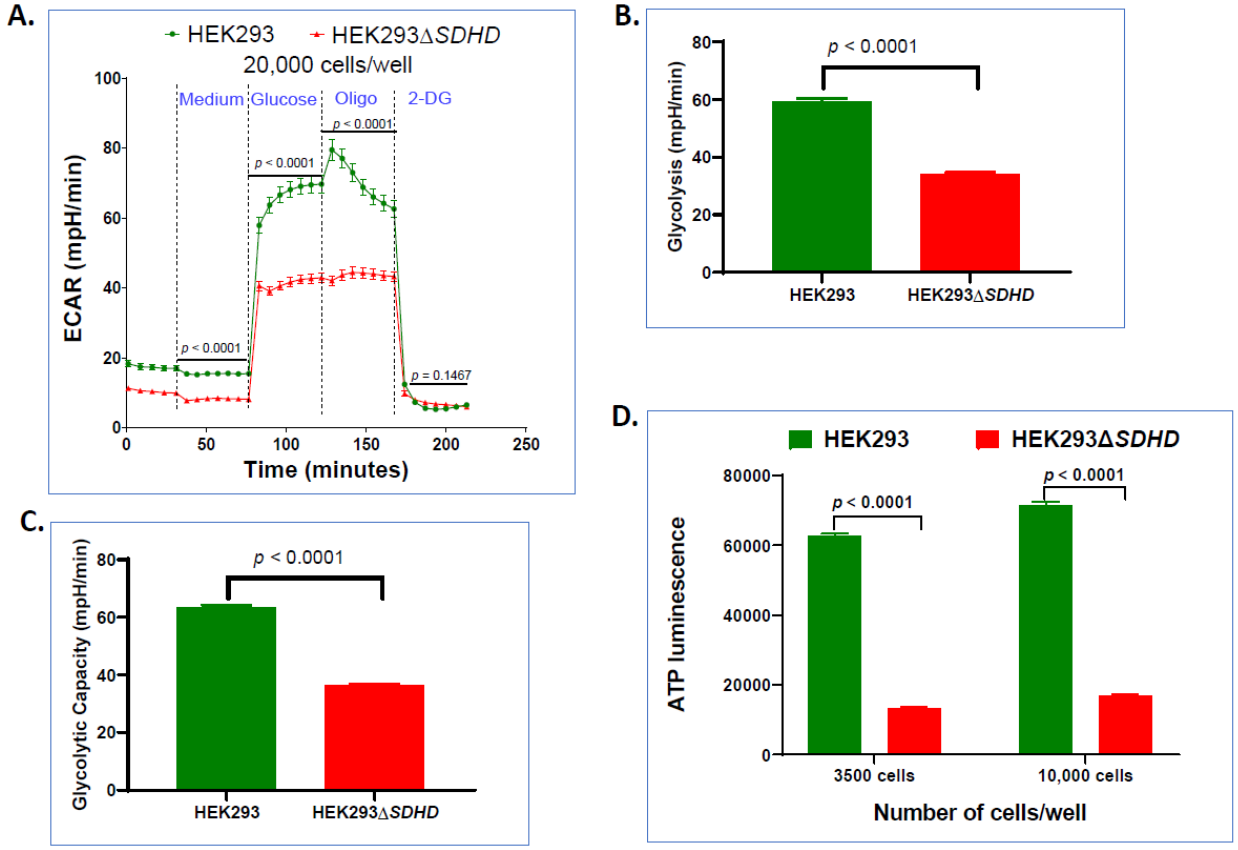

Figure 5. Glycolysis and ATP synthesis of cell lines. ECAR measured using Agilent Seahorse XFe96 analyzer of 20,000 live cells/well (A), and calculated glycolysis (B) and glycolytic capacity (C) are shown. The mean values were compared between the parent HEK293 and the mutant HEK293Δ*SDHD*. ATP synthesis of parent and mutant cells measured using Mitochondrial ToxGlo Assay (D) is shown. The measurements are expressed as total luminescence per 3500 or 10,000 cells. Error bars represent the SE of the mean.

($p < 0.0001$; Fig. 5B) and glycolytic capacity ($p < 0.0001$; Fig. 5C) decreased significantly in mutant cells. The findings indicate an association between SDHD function and glycolysis. The mutant cells produced significantly less ATP than parent cells at two different cell densities ($p < 0.0001$

when 3500 or 10,000 cells/well were used; Fig. 5D). Impaired ATP synthesis was consistent with suppressed mitochondrial and glycolytic metabolism.

2.6. Improved respiration and growth in HEK293Δ*SDHD* mutant cells treated with mitochondrial therapeutic idebenone. Idebenone is a short-chain benzoquinone with greater hydrophilicity [9], which has shown promise as a therapeutic for mitochondrial dysfunction [9-11]. We tested whether idebenone modified oxygen consumption of mutant HEK293Δ*SDHD* cells by Seahorse XFe96 and O2k respirometry O2k. In Seahorse assay, treatment of permeabilized mutant cells with 1 µM idebenone significantly increased basal respiration ($p < 0.0001$; Fig. 4C) and maximal respiratory capacity ($p < 0.0001$; Fig. 4E), but not reserved respiratory capacity ($p = 0.8847$; Fig. 4D). In O2k respirometry assay, G/M, rotenone, and succinate elicited no differences in respiration of mutant cells (Fig. 6A). In the presence of succinate, idebenone was incrementally added 10 minutes apart, with concentrations of 1 µM, following by three subsequent injections of 5 µM each. Compared to vehicle (DMSO), 1 µM idebenone elicited a non-statistically significant increase in oxygen consumption ($p = 0.1250$; Fig. 6A). Subsequent dose of 5 µM idebenone significantly increased oxygen consumption compared to vehicle in mutant cells ($p = 0.0119$), which peaked after the second dose of 5 µM idebenone ($p = 0.0508$; Fig. 6A). After the final injection of 5 µM idebenone, OXPHOS capacity was measured by adding ADP. Idebenone treated mutant cells had significantly improved OXPHOS capacity compared to the DMSO treated cells ($p = 0.0148$) (Fig. 4A).

We next investigated whether long-term idebenone treatment would influence cell growth. Due to the slow growth of HEK293Δ*SDHD* cells (Fig. 6B), cells were grown for 10 days in growth media where either 1, 5, or 10 µM idebenone was added to the media. After 10 days, 25.4% more cells were recovered from cells treated with 1 µM idebenone compared to the DMSO control ($p = 0.00959$; Fig. 6B). However, treatment with 5 µM idebenone did not improve growth of the mutant ($p = 0.9433$; Fig. 6B), whereas treatment with 10 µM idebenone caused cell death (not shown).

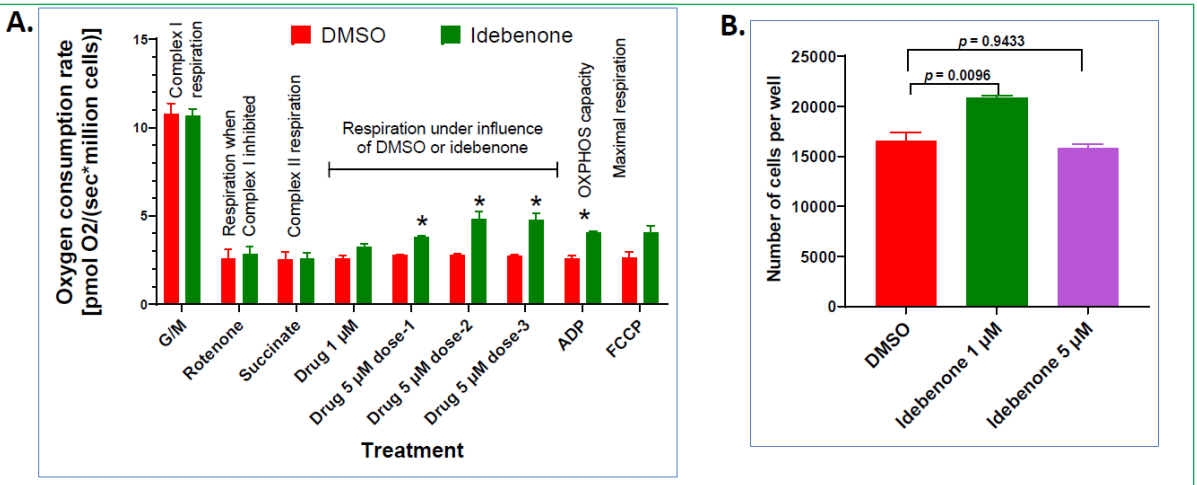

Figure 6. Restoring the defects of the mutant with use of the mitochondrial therapeutic idebenone. The oxygen consumption rates of permeabilized cells treated with DMSO or idebenone are shown (A). The rates per million cells in response to injection of substrates, inhibitor, or drug are depicted. The mean oxygen consumption values were compared between the idebenone treatment and DMSO control. The *p* values for the differences between the mean values of DMSO control versus idebenone treatment were 0.8689, 0.7605, 0.9394, 0.1250, 0.0119, 0.0508, 0.0323, 0.0148, and 0.1084 respectively for G/M, rotenone, succinate, 1 µM idebenone, 1st dose of 5 µM idebenone, 2nd dose of 5 µM idebenone, 3rd dose of 5 µM idebenone, ADP, and FCCP. The number of cells recovered from the mutant cultures treated with 1 µM idebenone or DMSO are shown (B). Error bars represent the SE of the mean.

3. DISCUSSION

Herein, we successfully used a CRISPR/Cas9 approach to mutate *SDHD*, a Complex II subunit in the inner-membrane region [1, 2], in HEK293 cells, generating the first such model to study the role of this essential Complex II subunit. Due to the role of Complex II in the ETC and Krebs cycle [1-3] as well as the association of SDHD mutations with disease pathologies [7], understanding the contribution of SDHD to cellular metabolism is warranted. Mutation in *SDHD* disrupted respiration all along the ETC, suppressed glycolysis and overall ATP synthesis, as well as limited cellular growth. Importantly, acute treatment with the synthetic ubiquinone analog idebenone was sufficient to improve Complex II-mediated mitochondrial respiration, OXPHOS capacity, and cell proliferation.

Predictably, mutation of SDHD inhibited Complex II-mediated respiration. Interestingly, however, mutation in SDHD significantly reduced Complex I-mediated respiration as well. Since Complex II drives Krebs cycle in a clock-wise direction by converting succinate to fumarate, we hypothesize

that mutation of SDHD slowed and/or disrupted Krebs cycle production of NADH, the substrate for Complex I. Mutation in SDHD also impaired OXPHOS capacity, maximal respiration, and ATP synthesis. Taken together, impairment in the SDHD subunit of Complex II is sufficient to impair overall ETC energy production.

Glycolysis, as determined by ECAR, was significantly reduced in HEK293Δ*SDHD* compared to parent cells. Reduced glycolysis may reflect a lower demand for pyruvate due to disrupted Krebs cycle as a result of mutation in SDHD, representing a potential negative feedback on glycolysis. Also, inhibition of mitochondrial respiration with oligomycin did not elicit a change in glycolysis in mutant cells, further reflecting impaired mitochondrial respiration. In addition to the suppressed metabolism, we also noted significantly slower growth in mutant cells compared to parent cells in culture media, which is likely reflective of the metabolic impairment in mutant cells.

Mutation of SDHD increased apoptosis and necrosis. The impaired glycolysis and mitochondrial respiration may have weakened the cell and cell membrane of the mutant making the cells more apoptotic and susceptible to necrosis. Quite interestingly, the long-term ROS generation declined as a result of SDHD mutation. In general, electrons that do not follow the normal order of the ETC pathway and instead leaked out are eventually transferred directly to O_2 to generate ROS [12, 13]. In our SDHD mutant, it is possible that impairment of clock-wise direction of Krebs cycle may have decreased the synthesis of NADH and $FADH_2$, the two electron donors to the ETC. Thus, limited donation of electrons may have led decreased electron transport through the ETC as well as decreased electron leakage out of the ETC giving rise to decreased ROS generation.

Finally, we explored whether SDHD mutation could be bypassed to improve some of the phenotypes observed. Idebenone, a short-chain benzoquinone that is more hydrophilic than ubiquinone [9], and has potential as a therapeutic for conditions associated with oxidative stress and mitochondrial dysfunction [9-11, 14-21]. Treatment with varying concentrations of idebenone improved Complex II-mediated oxygen consumption and OXPHOS capacity, suggesting that the

ubiquinone analog idebenone is able to substitute for Complex II as an electron donor to improve ETC function. Interestingly, long-term treatment with 1 μM of idebenone increased cell proliferation in HEK293Δ*SDHD* cells whereas 5 μM did not. Idebenone is known to have cell-type specific effects on cell proliferation [22-24]. While an increase in cell proliferation in our mutant HEK293Δ*SDHD* cells with idebenone is likely a result of improved substrate utilization, cell type should be taken into consideration for mitochondrial targeted therapies as to how other process may be influenced.

4. CONCLUSIONS

We generated a novel mutant of the Complex II subunit SDHD via CRISPR/Cas9 that resulted in severe augmentation to mitochondrial respiration and cell metabolism as well as suppressed growth. This novel tool could be valuable for testing potential mitochondrial-focused therapeutics as well as elucidating other mechanisms regulated by Complex II function.

5. MATERIALS AND METHODS

5.1. Cell lines and culture conditions. Human embryonic kidney cell line 293 (HEK293) was kindly provided by Dr. Joseph Ruiz at Enzerna Biosciences (Raleigh, NC). Media and reagents for growing and maintaining cells were purchased from Life Technologies Corporation (Carlsbad, CA). The cells were maintained in Dulbecco's Modified Eagle's medium (DMEM) supplemented with 10% (by volume) fetal bovine serum and 1% penicillin-streptomycin. Cells were sustained in a humidified incubator at 37ºC and 5% CO_2. A 0.25% trypsin-EDTA solution was used for detachment of cells. One Shot Stbl3 Chemically Competent cells of *Escherichia coli* (Life Technologies Corporation) were used for constructing the mutagenesis plasmid. Bacteria carrying

the plasmids were maintained in Luria Bertani (Sigma-Aldrich, St. Louis, MO) agar or broth, and sustained in a humidified incubator at 37ºC.

5.2. Construction and validation of *SDHD* mutant. Top and bottom sgRNA sequences for SDHD site were designed and purchased from Integrated DNA Technologies (Skokie, IL). sgRNA oligonucleotides were cloned into plasmid px458 (Addgene, Watertown, MA) and HEK293 cells were transfected with recombinant px458 plasmid using transfection reagent Xfect (Takara Bio USA Inc, Mountain View, CA). Clones with mutation in *SDHD* were picked using procedures described elsewhere [25]. Disruption of SDHD synthesis was validated by Western Immuno-blotting using rabbit polyclonal antibody SDHD (1:1000 in blocking buffer) (Cat# LS-C345301-100; LifeSpan Biosciences Inc, Seattle, WA) and rabbit polyclonal antibodies to β-Actin (1:10,000) (Cat# ab8227, Abcam Inc, Cambridge, MA). A clone missing the protein bands representing SDHD was chosen for further work and designated as HEK293Δ*SDHD* (Fig. 1).

5.3. Cell growth and metabolism. Aliquots of 100,000 cells of the parent HEK293 and the mutant HEK293Δ*SDHD* were introduced into 75 cm^2 flasks each carrying 25 ml growth media. After 4 days of incubation, cell numbers were quantified in triplicates. Generation of reactive oxygen species (ROS) was measured using ROS-Glo H_2O_2 Assay (Cat# G8820; Promega Corporation, Madison, WI). Apoptosis and necrosis were assessed using RealTime-Glo Annexin V Apoptosis and Necrosis Assay (Cat# JA1011; Promega). Extracellular Acidification Rate (ECAR) was determined with an Agilent Seahorse XFe96 analyzer [26, 27], and glycolysis and glycolytic capacity were calculated as described elsewhere [27]. Oxygen Consumption Rate (OCR) of saponin-permeabilized cells was assayed with an Agilent Seahorse XFe96 analyzer, and basal respiration, reserve respiratory capacity and maximal respiratory capacity were calculated as described elsewhere [27]. Oxygen consumption of saponin-permeabilized cells [28] was also measured by Oroboros O2k respirometry [29, 30]. Cellular ATP pool was measured using Mitochondrial ToxGlo Assay (Promega Corporation, Madison, WI).

5.4. Restoring the impaired growth and respiration the mutant. Effectiveness of the potential mitochondrial therapeutic idebenone in restoring the growth defects of the mutant HEK293Δ*SDHD* was evaluated. In this procedure, mutant cells were cultured on 6-well plates at 2000 cells/well in DMEM medium supplemented 1, 5, or 10 µM of idebenone. Fresh media containing the drug was added on days 3, 6 and 9, and the cell counts in wells of triplicates was determined following 10 days incubation. Efficacy of idebenone in improving respiration of permeabilized mutant cells was measured by O2k respirometry as described above with the following modification: subsequent to succinate injection, idebenone was injected into chambers at 1 or 5 µM final concentration. The control groups received DMSO. Moreover, effectiveness of idebenone in improving OCR of permeabilized cells was assessed with the Agilent Seahorse XFe96 analyzer as outlined above with the following modification: cells grown overnight in XFe96 culture plates were washed, and glucose-free DMEM (pH 7.4) supplemented with 10 mM glucose, 10 mM sodium pyruvate, and 2 mM glutamine, 20 µg/ml saponin and 1 µM of idebenone was added to the wells prior to incubating for 40 min at 37ºC in a CO_2-free station. The control wells received the same medium added with DMSO but without idebenone.

5.5. Statistical analyses. Student's t-tests were performed using Microsoft Excel program (Microsoft, Redmond, WA) or GraphPad Prism 7 (GraphPad Software, San Diego, CA) to compare the means of the parent versus mutant or vehicle control versus idebenone treatment. The ECAR data were analyzed by repeated measures ANOVA using GraphPad Prism 8. Mean differences between groups were considered statistically significant at $p < 0.05$.

LIST OF ABBREVIATIONS

Electron transport chain (ETC), Succinate dehydrogenase subunit D (SDHD), oxidative phosphorylation (OXPHOS), adenosine triphosphate (ATP), clustered regularly interspaced short

palindromic repeats/CRISPR-associated protein 9 (CRISPR/Cas9), dimethyl sulfoxide (DMSO), reactive oxygen species (ROS), oxygen consumption rate (OCR).

DECLARATIONS

Ethics approval and consent to participate: Not applicable.

Consent for publication: Not applicable.

Availability of data and materials: All data generated or analyzed during this study are included in this published article. Any additional data generated during the current study are available from the corresponding author on reasonable request.

Competing interests: Authors declare no competing interests.

Funding: This study was funded by Start-up Funds from Virginia Tech to D.A.B. (VT Fund #235170) and Start-up Funds from Virginia Tech (VT fund #178736) and NIH (R00AG057825-03) to J.C.D. We also thank members of the Brown and Drake labs for helpful discussion and feedback.

Authors' contributions: A.B.B. and D.A.B. conceived and planned the study. A.B.B. constructed the mutant and ran the assays. A.B.B. and J.C.D. analyzed the data, interpreted the results, and wrote the manuscript.

Acknowledgements: The authors would like to thank Dr. Joseph Ruiz of Enzerna Biosciences for the mammalian cell line HEK293, Nicholas Catanzaro of the Virginia Maryland College of Veterinary Medicine (VMCVM) for the valuable support with western immuno-blotting, Harini Sooryanarain of VMCVM for the support with the fluorescence and luminescence assays, Alex Thomson and Michael Allen of the Department of Human Nutrition, Foods & Exercise (HNFE) for

the support with Seahorse assay, and Justin Perry and Grace Davis of HNFE for the support with Oroboros O2k.

REFERENCES

1. Cecchini G: **Function and structure of complex II of the respiratory chain**. *Annu Rev Biochem* 2003, **72**:77-109.
2. Sun F, Huo X, Zhai Y, Wang A, Xu J, Su D, Bartlam M, Rao Z: **Crystal structure of mitochondrial respiratory membrane protein complex II**. *Cell* 2005, **121**(7):1043-1057.
3. Miyadera H, Shiomi K, Ui H, Yamaguchi Y, Masuma R, Tomoda H, Miyoshi H, Osanai A, Kita K, Omura S: **Atpenins, potent and specific inhibitors of mitochondrial complex II (succinate-ubiquinone oxidoreductase)**. *Proc Natl Acad Sci U S A* 2003, **100**(2):473-477.
4. Bourgeron T, Rustin P, Chretien D, Birch-Machin M, Bourgeois M, Viegas-Pequignot E, Munnich A, Rotig A: **Mutation of a nuclear succinate dehydrogenase gene results in mitochondrial respiratory chain deficiency**. *Nat Genet* 1995, **11**(2):144-149.
5. Astuti D, Latif F, Dallol A, Dahia PL, Douglas F, George E, Skoldberg F, Husebye ES, Eng C, Maher ER: **Gene mutations in the succinate dehydrogenase subunit SDHB cause susceptibility to familial pheochromocytoma and to familial paraganglioma**. *Am J Hum Genet* 2001, **69**(1):49-54.
6. Niemann S, Muller U: **Mutations in SDHC cause autosomal dominant paraganglioma, type 3**. *Nat Genet* 2000, **26**(3):268-270.
7. Baysal BE, Ferrell RE, Willett-Brozick JE, Lawrence EC, Myssiorek D, Bosch A, van der Mey A, Taschner PE, Rubinstein WS, Myers EN *et al*: **Mutations in SDHD, a mitochondrial complex II gene, in hereditary paraganglioma**. *Science* 2000, **287**(5454):848-851.
8. Bezawork-Geleta A, Rohlena J, Dong L, Pacak K, Neuzil J: **Mitochondrial Complex II: At the Crossroads**. *Trends Biochem Sci* 2017, **42**(4):312-325.
9. Erb M, Hoffmann-Enger B, Deppe H, Soeberdt M, Haefeli RH, Rummey C, Feurer A, Gueven N: **Features of idebenone and related short-chain quinones that rescue ATP levels under conditions of impaired mitochondrial complex I**. *PLoS One* 2012, **7**(4):e36153.
10. Haefeli RH, Erb M, Gemperli AC, Robay D, Courdier Fruh I, Anklin C, Dallmann R, Gueven N: **NQO1-dependent redox cycling of idebenone: effects on cellular redox potential and energy levels**. *PLoS One* 2011, **6**(3):e17963.
11. Heitz FD, Erb M, Anklin C, Robay D, Pernet V, Gueven N: **Idebenone protects against retinal damage and loss of vision in a mouse model of Leber's hereditary optic neuropathy**. *PLoS One* 2012, **7**(9):e45182.
12. Turrens JF: **Mitochondrial formation of reactive oxygen species**. *J Physiol* 2003, **552**(Pt 2):335-344.
13. Cadenas E, Davies KJ: **Mitochondrial free radical generation, oxidative stress, and aging**. *Free Radic Biol Med* 2000, **29**(3-4):222-230.
14. Palecek T, Fikrle M, Nemecek E, Bauerova L, Kuchynka P, Louch WE, Spicka I, Rysava R: **Contemporary treatment of amyloid heart disease**. *Curr Pharm Des* 2015, **21**(4):491-506.
15. Strawser CJ, Schadt KA, Lynch DR: **Therapeutic approaches for the treatment of Friedreich's ataxia**. *Expert Rev Neurother* 2014, **14**(8):949-957.

16. Lynch DR, Perlman SL, Meier T: **A phase 3, double-blind, placebo-controlled trial of idebenone in friedreich ataxia**. *Arch Neurol* 2010, **67**(8):941-947.
17. Buyse GM, Goemans N, van den Hauwe M, Thijs D, de Groot IJ, Schara U, Ceulemans B, Meier T, Mertens L: **Idebenone as a novel, therapeutic approach for Duchenne muscular dystrophy: results from a 12 month, double-blind, randomized placebo-controlled trial**. *Neuromuscul Disord* 2011, **21**(6):396-405.
18. Buyse GM, Voit T, Schara U, Straathof CS, D'Angelo MG, Bernert G, Cuisset JM, Finkel RS, Goemans N, Rummey C *et al*: **Treatment effect of idebenone on inspiratory function in patients with Duchenne muscular dystrophy**. *Pediatr Pulmonol* 2017, **52**(4):508-515.
19. McDonald CM, Meier T, Voit T, Schara U, Straathof CS, D'Angelo MG, Bernert G, Cuisset JM, Finkel RS, Goemans N *et al*: **Idebenone reduces respiratory complications in patients with Duchenne muscular dystrophy**. *Neuromuscul Disord* 2016, **26**(8):473-480.
20. Buyse GM, Voit T, Schara U, Straathof CSM, D'Angelo MG, Bernert G, Cuisset JM, Finkel RS, Goemans N, McDonald CM *et al*: **Efficacy of idebenone on respiratory function in patients with Duchenne muscular dystrophy not using glucocorticoids (DELOS): a double-blind randomised placebo-controlled phase 3 trial**. *Lancet* 2015, **385**(9979):1748-1757.
21. Fiebiger SM, Bros H, Grobosch T, Janssen A, Chanvillard C, Paul F, Dorr J, Millward JM, Infante-Duarte C: **The antioxidant idebenone fails to prevent or attenuate chronic experimental autoimmune encephalomyelitis in the mouse**. *J Neuroimmunol* 2013, **262**(1-2):66-71.
22. Seo Y, Park J, Kim M, Lee HK, Kim JH, Jeong JH, Namkung W: **Inhibition of ANO1/TMEM16A Chloride Channel by Idebenone and Its Cytotoxicity to Cancer Cell Lines**. *PLoS One* 2015, **10**(7):e0133656.
23. Augustyniak J, Lenart J, Zychowicz M, Stepien PP, Buzanska L: **Mitochondrial biogenesis and neural differentiation of human iPSC is modulated by idebenone in a developmental stage-dependent manner**. *Biogerontology* 2017, **18**(4):665-677.
24. Zhang J, Zhang J, Li T, Zhang N, Tang S, Tao Z, Zhou X, Sun X, Chen H: **Effect of idebenone on bone marrow mesenchymal stem cells in vitro**. *Mol Med Rep* 2018, **17**(4):5376-5383.
25. Ran FA, Hsu PD, Wright J, Agarwala V, Scott DA, Zhang F: **Genome engineering using the CRISPR-Cas9 system**. *Nat Protoc* 2013, **8**(11):2281-2308.
26. Ryall JG: **Simultaneous Measurement of Mitochondrial and Glycolytic Activity in Quiescent Muscle Stem Cells**. *Methods Mol Biol* 2017, **1556**:245-253.
27. Rafikov R, Sun X, Rafikova O, Louise Meadows M, Desai AA, Khalpey Z, Yuan JX, Fineman JR, Black SM: **Complex I dysfunction underlies the glycolytic switch in pulmonary hypertensive smooth muscle cells**. *Redox Biol* 2015, **6**:278-286.
28. Hahn D, Kumar RA, Ryan TE, Ferreira LF: **Mitochondrial respiration and H2O2 emission in saponin-permeabilized murine diaphragm fibers: optimization of fiber separation and comparison to limb muscle**. *Am J Physiol Cell Physiol* 2019, **317**(4):C665-C673.
29. Alleman RJ, Tsang AM, Ryan TE, Patteson DJ, McClung JM, Spangenburg EE, Shaikh SR, Neufer PD, Brown DA: **Exercise-induced protection against reperfusion arrhythmia involves stabilization of mitochondrial energetics**. *Am J Physiol Heart Circ Physiol* 2016, **310**(10):H1360-1370.
30. Goswami I, Perry JB, Allen ME, Brown DA, von Spakovsky MR, Verbridge SS: **Influence of Pulsed Electric Fields and Mitochondria-Cytoskeleton Interactions on Cell Respiration**. *Biophys J* 2018, **114**(12):2951-2964.

Figures

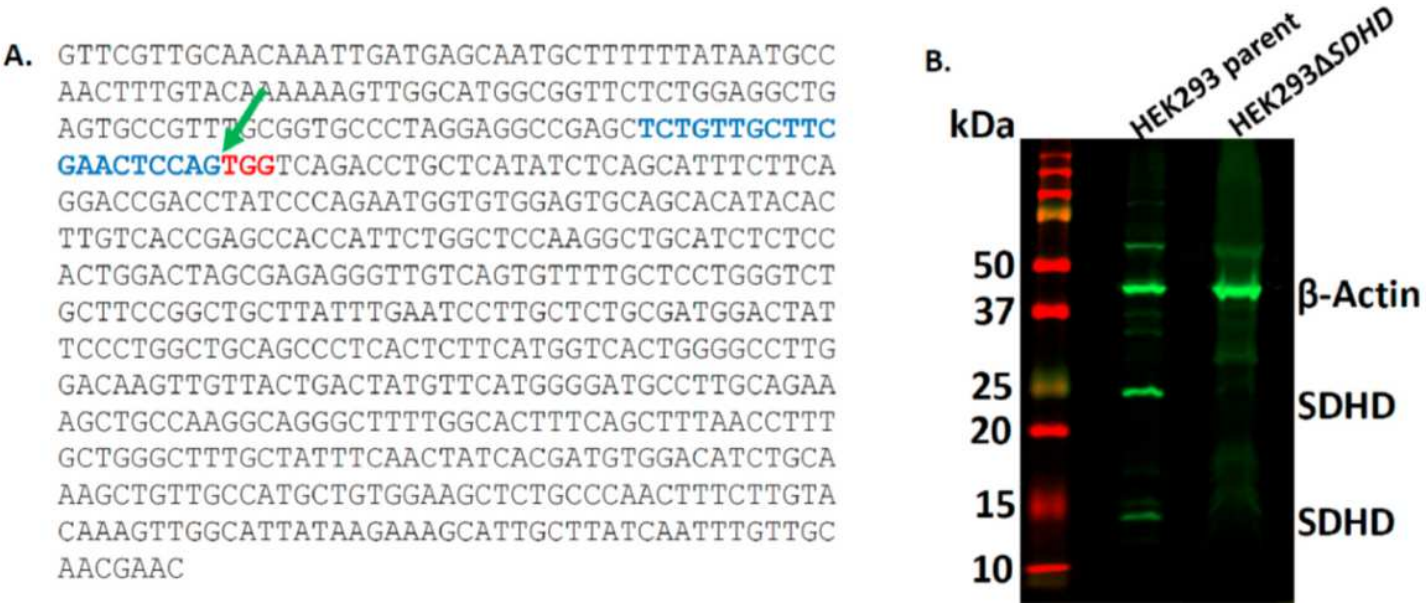

Figure 1

Construction of the SDHD mutant. The gene sequence of SDHD with CRISPR targeting sites is shown (A). The sgRNA and PAM sequences predicted by the online idtdna program are depicted in blue and red colors, respectively; the specific site for mutation (at 118-bp) is shown with a green arrow. Expression of SDHD protein is shown (B). The protein extracts reacted with rabbit polyclonal antibodies to SDHD and rabbit polyclonal antibodies to β-Actin are shown.

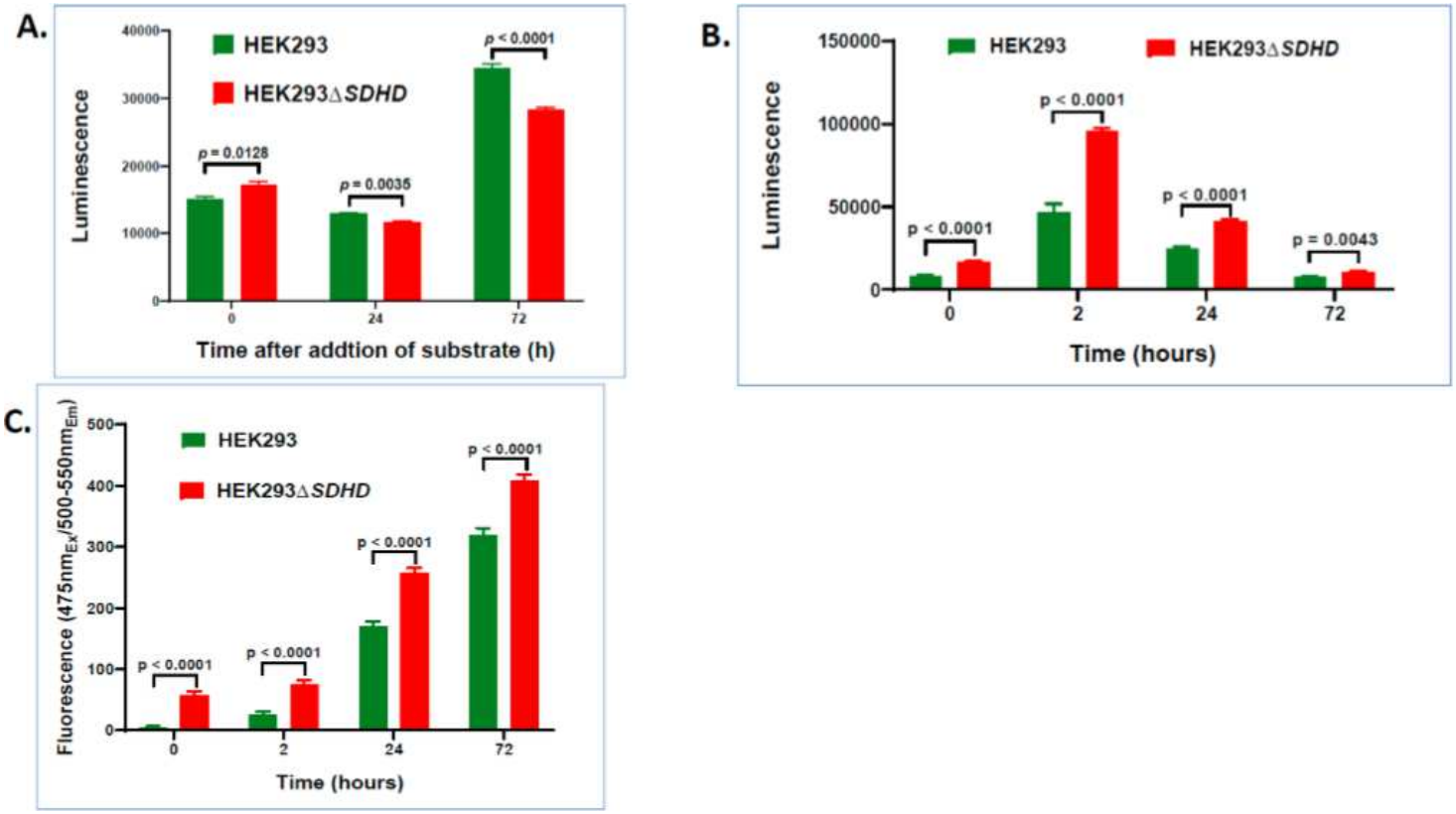

Figure 2

ROS production, apoptosis, and necrosis of cell lines. ROS generation measured using ROS-Glo H2O2, Assay of parent HEK293 and the mutant HEK293ΔSDHD is shown (A). The measurements are expressed as total luminescence per 15,000 cells measured at at 0, 24, and 72 hours after addition of substrate to the reaction. Apoptosis (B) and necrosis (C) per 15,000 cells measured using RealTime-Glo Annexin V Apoptosis and Necrosis Assay at 0, 2, 24, and 72 hours of incubation are shown. The apoptosis measurements are expressed as total luminescence, whereas necrosis measurements expressed as total fluorescence. Error bars represent the SE of the mean.

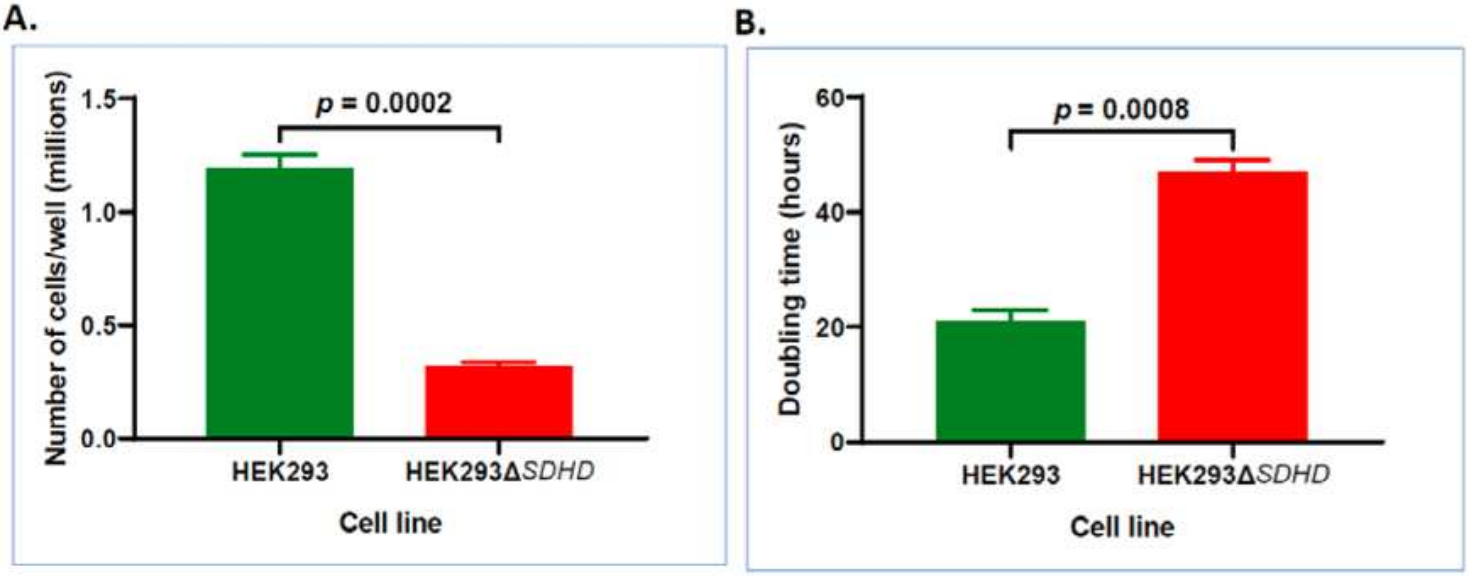

Figure 3

Growth of cell lines. The number of cells harvested from the parent HEK293 and the mutant HEK293ΔSDHD cells after four days of culture (A) and doubling times of cells (B) are shown. Error bars represent the SE of the mean.

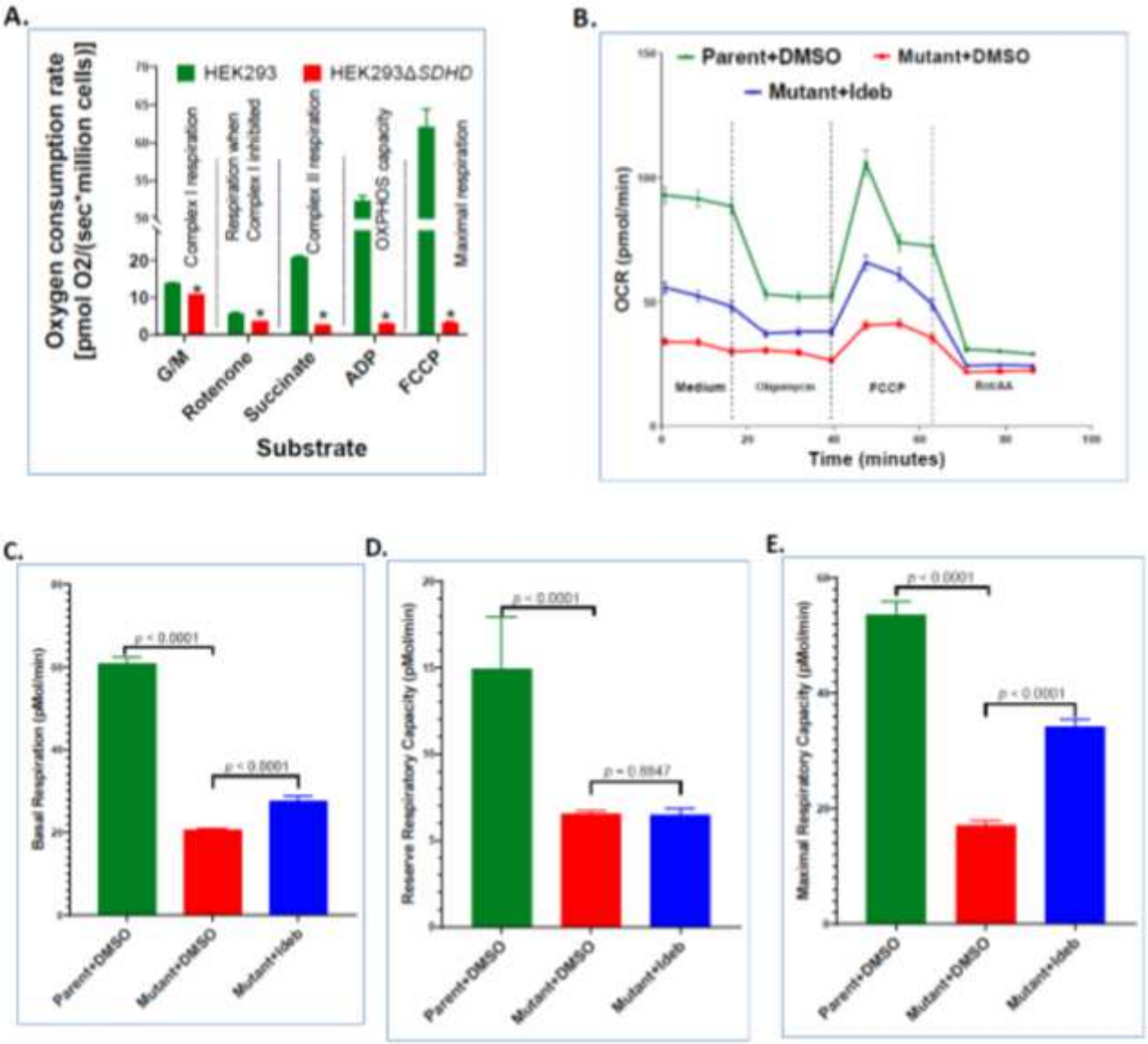

Figure 4

Respiration, of cell lines. Oxygen consumption rates measured using Croboros O2k per million cells in response to treatment with glutamate-malate (G/M), rotenone, succinate, ADP. and FCCP (A) are shown. The mean oxygen consumption rates were compared between the parent HEK293 and the mutant HEK293ΔSDHD. The p values for the differences between the mean values were 0.0019, 0.0101, 0.0002, 0.0002, and 0.0017, respectively for Complex | respiration, rotenone treatment, Complex II respiration, OXPHOS capacity. and maximal respiration. Oxygen consumption rate (OCR) was measured using Agilent Seahorse XFe96 of parent cells treated DMSO (Parent+tDMSO), mutant cells treated DMSO Mutant+DMSO), and mutant cells treated 1M idebenone (Mutant+Ideb). OCR per 20.000 permeabilized cells (B), and the calculated basal respiration (C). reserve respiratory capacity (D) and maximal respiratory capacity (E) are shown. The mean OCR values were compared between the parent versus the mutant or DMSO treatment versus idebenone treatment. Error bars represent the SE of the mean.

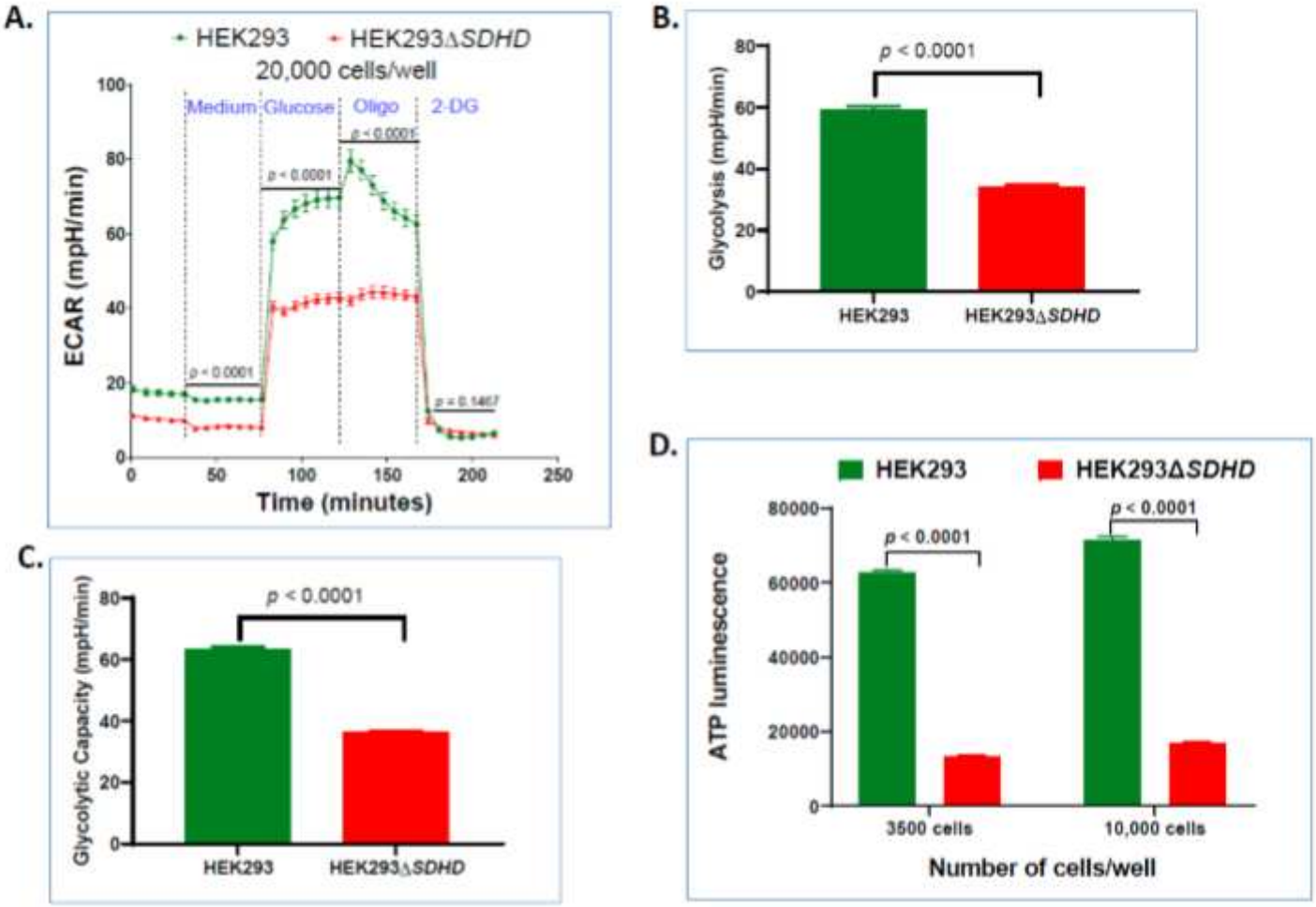

Figure 5

Glycolysis and ATP synthesis of cell lines. ECAR measured using Agilent Seahorse XFe96 analyzer of 20,000 live cells/well (A), and calculated glycolysis (B) and glycolytic capacity (C) are shown. The mean values were compared between the parent HEK293 and the mutant HEK293ΔSDHD. ATP synthesis of parent and mutant cells measured using Mitochondrial ToxGlo Assay (D) is shown. The measurements are expressed as total luminescence per 3500 or 10,000 cells. Error bars represent the SE of the mean.

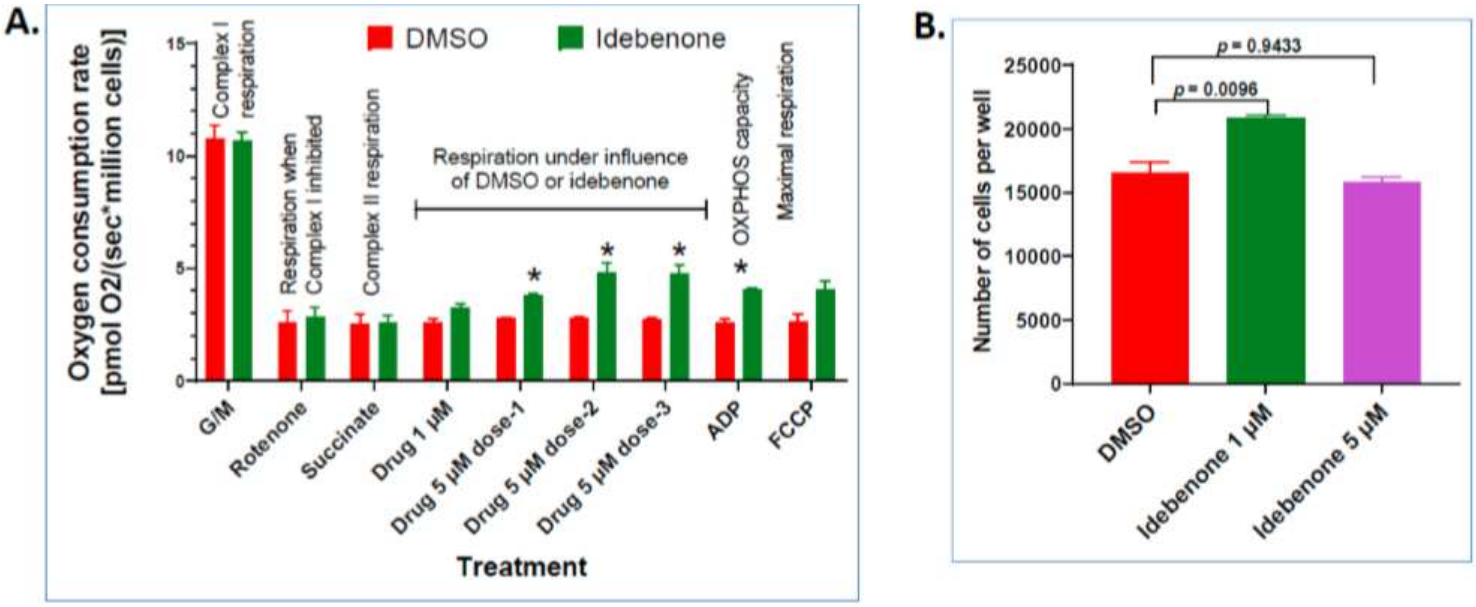

Figure 6

Restoring the defects of the mutant with use of the mitochondrial therapeutic idebenone. The oxygen consumption rates of permeabilized cells treated with DMSO or idebenone are shown (A). The rates per million cells in response to injection of substrates, inhibitor, or drug are depicted. The mean oxygen consumption values were compared between the idebenone treatment and DMSO control. The p values for the differences between the mean values of DMSO control versus idebenone treatment were 0.8689, 0.7605, 0.9394. 0.1250, 0.0119, 0.0508, 0.0323, 0.0148. and 0.1084 respectively for G/M, rotenone, succinate, 1 µM idebenone. 1st dose of 5 µM idebenone, 2nd dose of 5 µM idebenone, 3rd dase of 5 µM idebenone, ADP, and FCCP. The number of cells recovered from the mutant cultures treated wth 1 µM idebenone or DMSO are shown (B). Error bars represent the SE of the mean.